

A One-Dimensional Model of a Turbulent Jet Diffusion Flame in an Ambient Atmospheric Flow, Derived from a Three-Dimensional Model

J. SERVERT, A. CRESPO* and J. HERNANDEZ†

*E. T. S. I. Industriales, Universidad Politécnica de Madrid,
José Gutiérrez Abascal, 2, 28006 Madrid, Spain*

(Received 1 November 1995; In final form 12 December 1996)

A rigorous deduction of a one-dimensional (1D) model of turbulent jet diffusion flames developed for releases of gaseous fuels is presented. This model considers the presence of a non-uniform incident wind and is derived from a full three-dimensional (3D) formulation of the fluid dynamics equations complemented with models for chemical reaction, thermal radiation and an adaptation of the $k-\epsilon-g$ closure method. To deduce the one-dimensional model, the 3D problem is considered to be parabolic along the center line of the flame and self-similar profiles in planes normal to this line are assumed. New terms, not present in previous works, have been introduced in the 1D conservation equations and an alternative approach to derive the production terms of the turbulent kinetic energy and of the mixture fraction variance is proposed. To evaluate the validity and usefulness of the model, its results have been compared with those of the three-dimensional model, developed by the authors, and with available wind-tunnel and full-scale experimental results, and a good agreement is found.

Keywords: Integral model; turbulent jet diffusion flames

1. INTRODUCTION

Turbulent jet fires are involved, either as a hazard or as a result of a controlled relief of flammable gases, in some operational or emergency situations. There are different ways to predict the effects of these fires. One is to use mathematical models based on the Navier-Stokes equations, complemented with some

*Corresponding author.

†E. T. S. I. Industriales, UNED, Ciudad Universitaria, 28040 Madrid.

appropriate models describing combustion and a closure procedure to model the turbulent transport terms. The numerical resolution of these models is commonly based on finite-differences approximations of the equations (Fairweather *et al.*, 1992; Hernández *et al.*, 1995), which may require a relatively large computational effort.

The flow equations can be simplified if appropriate averages and distribution profiles can be defined in planes normal to a center line. Then, the partial differential equations may be converted to ordinary differential equations, with the distance along the center line as independent variable. The problem is then simpler and the computer time is substantially reduced, from hours to fractions of minutes. This type of one-dimensional or integral model has been used extensively by Escudier (1972), Fay (1973), Tamanini (1981), Peters and Göttgens (1991), Cook (1991), and Caulfield *et al.* (1993), among others. In this work, we present a rigorous way to derive the one-dimensional equations, that, in our knowledge, has not previously been formulated. A more detailed description of the derivation of this model can be found in Servet (1993), and Crespo *et al.* (1994). Fay (1973) proposed a model somehow similar to ours, but it has a more complex interpretation and introduces a definition of the average quantities that depends on the existence of an ambient wind. Ours applies to situations in which there is both ambient wind with shear and no wind. Whereas other models (Escudier, 1972; Cook, 1991; Caulfield *et al.*, 1993; Tamanini, 1981) either assume top-hat profiles or cosine-type profiles that end at a finite distance from the center line, the model presented here can also be applied using self-similar profiles that extend to infinity in the transverse direction.

The three-dimensional equations describing the flow field are formulated assuming that the flow is parabolic along the center line. The k - ϵ - g model is used to close the turbulent equations, and additional equations for the mixture fraction and its variance are formulated. The combustion model is based on an infinitely-fast reaction mechanism and a prescribed shape for the probability-density function of the mixture fraction. Mass fractions of fuel, carbon dioxide and water vapor are obtained as functions of the mixture fraction and its variance, and the temperature is determined as a function of these same variables and of the enthalpy. A separate method, similar to the one proposed by Caulfield *et al.* (1993), is used to calculate the soot mass fraction. The method proposed by Modak (1979) is used to evaluate the emissivity of the mixture from the mass fractions of CO_2 , H_2O and soot that is needed to calculate radiation losses.

Integrating the three-dimensional equations in cross sections and applying a spatial average, the one-dimensional equations are obtained. If the turbulent

diffusivities of all the variables are equal, a single relationship between the average and maximum values of the quantities is obtained that simplifies the numerical calculation, in particular the calculation of the source terms.

Further manipulation of both the one-dimensional and the three-dimensional equations leads to a generalization of Tamanini's (1981) expression for the production term of the turbulent kinetic energy and of the variance of the mixture fraction, that takes into account the cross-wind effect, and extends its validity to arbitrary spatial distributions.

A code, termed UPMFIRE, has been developed to implement the one-dimensional model proposed here. The results of the code are compared with wind-tunnel experimental results (Duijm, 1993; Verheij and Duijm, 1991; Bakkum, 1994) and with full-scale measurements (Ott, 1993; Bennett *et al.*, 1991). The model has also been compared with a three-dimensional model (Hernández *et al.*, 1995). In general, a good agreement has been found from these comparisons, and this code can be considered as a useful tool in risk assessment.

To design and operate some industrial facilities where jet fires can occur, information about the heat transferred to surroundings objects or engulfed obstacles is also needed. A method to include the effect of an engulfed obstacle, small in comparison with the characteristic length of the flame, by means of a finite jump in the flow conditions, is described by Crespo *et al.* (1994), Crespo *et al.* (1995) and Servert *et al.* (1995), and will not be considered here. Other effects included in this 1D code (Crespo *et al.*, 1994), not presented here, are the estimation of lift-off distance and of the equivalent exit conditions for under-expanded jets.

2. FLOW EQUATIONS

The one-dimensional conservation equations of mass, momentum, energy, mixture fraction, ξ , turbulent kinetic energy, k , dissipation rate of the turbulent kinetic energy, ε , and variance of the mixture fraction, g , are obtained from the classical three-dimensional equations described for example in Fairweather *et al.* (1992) and Hernández *et al.* (1995). The magnitudes k and ε are needed to close the turbulent transport terms, and ξ and g to model combustion. The equations may be written in the general form

$$\frac{\partial \bar{\rho} \tilde{\phi}}{\partial t} + \frac{\partial}{\partial x_i} (\bar{\rho} \tilde{v}_i \tilde{\phi} - \Gamma_{\phi_i}) = S_{\phi} \quad (1)$$

where $\tilde{\phi}$ can be equal to: 1, any component of the velocity, \tilde{v}_i , total enthalpy, \tilde{h} , mixture fraction, $\tilde{\xi}$, turbulent kinetic energy, k , dissipation rate of the turbulent kinetic energy, ε , or variance of the mixture fraction, g . In this equation, $\bar{\rho}$ is the density and S_ϕ is the source term. The Favre average is denoted by a tilde and the temporal average by a dash. The averaged magnitudes will be assumed to be steady, so that the first term in the left-hand side of equation (1) will be zero. The diffusion vector is expressed in the following way for the scalar variables:

$$\Gamma_{\phi_i} = \frac{\mu_t}{\sigma_\phi \bar{\rho}} \frac{\partial \tilde{\phi}}{\partial x_i}, \quad (2)$$

and for the turbulent Reynolds stresses:

$$\tau_{ij} = \mu_t \left(\frac{\partial \tilde{v}_i}{\partial x_j} + \frac{\partial \tilde{v}_j}{\partial x_i} \right) - \frac{2}{3} \delta_{ij} \left(\mu_t \frac{\partial \tilde{v}_k}{\partial x_k} + \bar{\rho} k \right), \quad (3)$$

where μ_t is the turbulent dynamic viscosity, and σ_ϕ is the turbulent Prandtl number for the variable ϕ . The turbulent viscosity is obtained from

$$\mu_t = C_\mu \bar{\rho} \frac{k^2}{\varepsilon}, \quad (4)$$

where C_μ is the classical coefficient of the k - ε model, that usually takes the value 0.09.

The source terms include buoyancy effects in the vertical momentum equation, and production and dissipation terms in the equations for k , ε and g . In the energy equation, the work of gravity force has been neglected and the Mach number has been assumed to be low enough so that the kinetic energy is negligible compared to the thermal energy; then, the only source term that is left is the one corresponding to thermal radiation.

The model is completed with a perfect gas law,

$$\frac{\bar{p}}{\bar{\rho}} = R_g \tilde{T}, \quad (5)$$

where the pressure is assumed to be constant, equal to the ambient pressure. Pressure variations are neglected compared with the value of the absolute

pressure. A state equation for enthalpy such as

$$d\tilde{h} = c_p d\tilde{T} + Q d\tilde{Y}_F, \quad (6)$$

where c_p can be a function of temperature and composition, is used.

3. COMBUSTION MODEL

To define the combustion model, the classical hypothesis of one-step, irreversible reaction (represented by Fuel + r_e Oxidizer \rightarrow (1 + r_e) Products, where r_e is the stoichiometric ratio), fast chemistry, and equal diffusivities for all the species are made. This leads to the classical conserved-scalar approach and to the well-known relation

$$Y_F(\xi) = \frac{\xi - \xi_s}{1 - \xi_s}; \quad \xi > \xi_s,$$

$$Y_F(\xi) = 0; \quad \xi \leq \xi_s, \quad (7)$$

where Y_F is the instantaneous value of the fuel mass fraction and ξ_s is the stoichiometric mixture fraction. From the instantaneous value, the Favre average is obtained through

$$\tilde{Y}_F = \frac{1}{1 - \xi_s} \int_{\xi_s}^1 (\xi - \xi_s) P(\xi) d\xi, \quad (8)$$

where $P(\xi)$ is the Favre-averaged probability density function of ξ of a predefined shape, whose parameters are expressed in terms of the average values of the mixture fraction and its variance, g . For the predefined shape of $P(\xi)$ a two-delta function has been used; also an alternative approach based on a correlation for the unmixedness integral (Mudford and Bilger, 1984) can be employed. A detailed explanation may be found in Hernández *et al.* (1995).

To calculate the temperature, equation (6) is used, where \tilde{Y}_F is obtained from equation (8) and \tilde{h} is calculated using the energy equation.

The instantaneous mass fractions of oxidizer and products are

$$Y_O = (r_e Y_F + Y_{Oa}) - \xi(r_e + Y_{Oa}), \quad (9)$$

$$Y_P = (r_e + 1)(\xi - Y_F). \quad (10)$$

If the composition of the hydrocarbon is given by C_nH_m and $\xi < \xi_s$, the products are mainly CO_2 and H_2O , whose mass fractions are obtained from stoichiometry:

$$Y_{H_2O} = 9(\xi - Y_F) \frac{m}{12n + m}, \quad (11)$$

$$Y_{CO_2} = 44(\xi - Y_F) \frac{n}{12n + m}. \quad (12)$$

Equations (9) to (12) are linear in both ξ and Y_F , and consequently also hold for the Favre averaged values.

Other products are assumed to have small mass fractions, and are not usually relevant except for soot, which is considered because it plays an important role in radiative processes, and for others, such as CO, because of its contaminant effects. Servet (1993) proposes a method to calculate CO mass fraction, based on a compilation of experimental results by Sivathanu and Faeth (1990), that will not be presented here.

A procedure for the calculation of soot mass fraction similar to the one proposed by Fairweather *et al.* (1991) and latter applied to 1D models by Caulfield *et al.* (1993) is used in this work. Fairweather *et al.* (1991) solve two conservation equations, similar to equation (1), one for the soot mass fraction and another for the particle number density. In the equation for soot mass fraction, source terms associated to nucleation, surface growth, and oxidation are included. The equation for particle number density includes source terms due to nucleation and coagulation. Soot formation proceeds from a pyrolysis intermediate, acetylene, that is considered to form solid carbon through nucleation and surface growth. Acetylene is obtained as a function of ξ , which has been evaluated by Fairweather *et al.* (1991) for laminar combustion using a 60 s^{-1} strain rate for CH_4 .

4. AMBIENT FLOW

The ambient flow where the jet diffuses corresponds to the surface layer of the atmospheric boundary layer in uniform, flat terrain. In this model, the ambient magnitudes satisfy equation (1) and are considered to change only with height (Crespo *et al.*, 1991). It is assumed that they vary in a characteristic length which is much larger than that corresponding to the variation of flame

properties in transverse direction. They are expressed in terms of the surface roughness of the ground, the Monin-Obukhov length (related to atmospheric stability), the turbulent friction velocity, and the flow properties at the ground. For the case of a neutral atmosphere, the Monin-Obukhov length is equal to infinity, and the corresponding expressions are: for the velocity,

$$v_a = v_{xa} = 2.5 u^* \log\left(\frac{z}{z_0}\right), \quad v_{ya} = 0, \quad v_{za} = 0; \quad (13)$$

for the turbulent kinetic energy and its dissipation rate,

$$k_a = \frac{u^{*2}}{C_\mu^{0.5}}, \quad \varepsilon_a = 2.5 \frac{u^{*3}}{z}, \quad (14)$$

and, for the mixture fraction and its variance, since there is no fuel in the ambient,

$$\xi_a = 0, \quad g_a = 0. \quad (15)$$

The detailed expressions for non-neutral atmospheres can be found in Crespo *et al.* (1991).

5. DEDUCTION OF THE ONE-DIMENSIONAL MODEL

For the flame described in the introduction and shown schematically in Figure 1, if a jet center line and self-similar profiles in planes normal to it can be defined, the partial differential equations presented in section 2 may be converted to ordinary differential equations, with the distance along the center line as the independent variable. The center line is assumed to be contained in a plane normal to the ground. It is also assumed that, in planes normal to the center line, the perturbations of all dependent variables, $|\tilde{\phi} - \phi_a|$, are largest at the center line itself, and that they decay and tend to zero for large enough values of the radial distance r to the center line. For all the dependent variables of equation (1), it is assumed that there are self-similar profiles of the form

$$\tilde{\phi} - \phi_a = (\phi_c - \phi_a) \psi_\phi\left(\frac{r}{R_\phi}, \varphi\right), \quad (16)$$

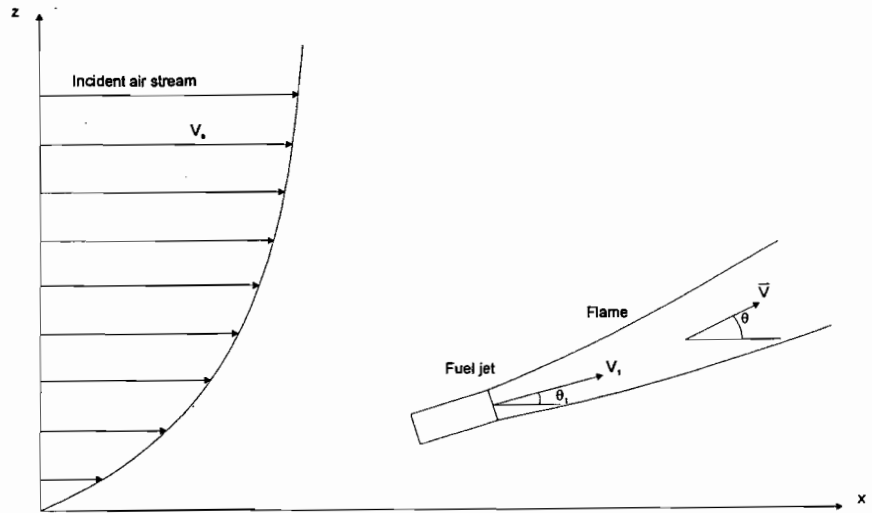


FIGURE 1 Schematic showing the model.

where ϕ is the azimuthal angle, and ψ_ϕ and R_ϕ satisfy the normalization conditions

$$\int_0^{2\pi} \int_0^\infty \psi_\phi r d\phi dr = \pi R_\phi^2, \quad \psi_\phi(0, \phi) = 1. \quad (17)$$

R_ϕ and ϕ_c are functions of the coordinate along the center line, s , to be calculated from the 1D model. This assumption may look inconsistent because, due to the curvature of the center-line, the planes normal to it would intersect and $\tilde{\phi}$ could be multiple-valued. However, because of the parabolic approximation, the radius of curvature of the center line, that is expected to be at least of the order of magnitude of its length, s , should be much larger than the characteristic length, R_ϕ , of decay of Ψ_ϕ , so that $\Psi_\phi \approx 0$ in the region where $\tilde{\phi}$ could be multivalued.

So far, all the selected profiles have axial symmetry. Buoyancy and lateral wind could make this assumption questionable, and this is a limitation to be relaxed in future works. The Gaussian distribution,

$$\Psi_\phi = \exp\left[\left(\frac{-r}{R_\phi}\right)^2\right], \quad (18)$$

is the one used to obtain the results presented in this work. For the exact solution of the laminar jet, that also holds for the turbulent jet, the distribution

is (Schlichting, 1968)

$$\Psi_\phi = \frac{1}{\left(1 + \left(\frac{r}{R_\phi}\right)^2\right)^2}. \quad (19)$$

Caulfield *et al.* (1993) use the cosine profile, that extends to a finite distance, $R_{1\phi}$:

$$\Psi_\phi = \frac{1}{2}(1 + \cos(\pi r/R_{1\phi})), \quad r < R_{1\phi}; \quad \Psi_\phi = 0, \quad r > R_{1\phi}$$

where

$$R_{1\phi} = \left(\frac{2\pi^2}{\pi^2 - 4}\right)^{1/2} R_\phi; \quad (20)$$

the normalization condition of equation (17) has been used to calculate the relationship between R_ϕ and $R_{1\phi}$.

5.1. Definition of the Spatial Averages

The following spatial-averages, denoted by $\langle \rangle$, are defined:

$$\dot{m}(\langle \tilde{\phi} \rangle - \phi_a) = \lim_{A \rightarrow \infty} \int_A \bar{\rho} \tilde{u} (\tilde{\phi} - \phi_a) dA, \quad (21)$$

where A is contained in a plane normal to the center line and $dA = r d\phi dr$. It is assumed that the average of the velocity component contained in that plane, $\langle \vec{w} \rangle$, is equal to zero, and that \tilde{u} is the velocity component normal to it. For large A , the value of $\tilde{\phi}$ is assumed to tend to ϕ_a rapidly enough, so that the integral is finite.

The mass flow rate, \dot{m} , across A is defined by

$$\dot{m} - \dot{m}_a = \lim_{A \rightarrow \infty} \int_A (\bar{\rho} \tilde{u} - \rho_a v_a \cos\theta) dA, \quad (22)$$

where θ is the angle that the center line forms with the horizontal plane, and \dot{m}_a is an equivalent mass flux of air through the cross section, that can not be defined as the integral $\int \rho_a v_a \cos \theta dA$ because it will diverge as A tends to infinity. The following expression is proposed for \dot{m}_a :

$$\dot{m}_a = \dot{m} \frac{\rho_a v_a \cos \theta}{\rho_m \langle \tilde{u} \rangle}. \quad (23)$$

The equivalent average density is defined using the equation of state

$$\rho_m = \frac{p_a}{R_g \langle \tilde{T} \rangle}, \quad (24)$$

where p_a is the ambient pressure, and equation (21) is used to evaluate $\langle \tilde{T} \rangle$, even though the temperature is not a dependent variable of equation (1), and has not a distribution of the form given by equation (16) except downstream of the flame tip ($\xi_c = \xi_{st}$), where the temperature is proportional to the enthalpy. Upstream of the flame tip the temperature has the maximum value at $r > 0$ (at the position where $\tilde{\xi} = \xi_{st}$ if radiation were neglected), even though the maximum of Ψ is for $r = 0$.

An equivalent flame radius is defined by

$$b = \sqrt{\frac{\dot{m}}{\rho_m \langle \tilde{u} \rangle \pi}}, \quad (25)$$

that coincides with R for a top-hat profile.

5.2. One-Dimensional Conservation Equations

To obtain the one-dimensional conservation equations, the following procedure is used. First, the general conservation equations (1) for the perturbed, $\tilde{\phi}$, and unperturbed, ϕ_a , flows are subtracted. The result is integrated over a control volume enclosed by two cross-sections of area A , separated by a very small distance ds , and a lateral surface where $r \gg R_\phi$ and therefore $\tilde{\phi} \approx \phi_a$. As indicated when discussing the validity of equation (16), the two cross-sections do not intersect. Using again the parabolic hypothesis, the sum of the turbulent diffusion fluxes over the two cross-sections can be neglected. On the other hand, if the difference between the perturbed and unperturbed turbulent diffusion fluxes decreases with radial distance faster than $1/r$, the integral of the

flux of the turbulent diffusion vector also vanishes over the lateral surface. Consequently, the turbulent diffusive flux will vanish over all the surfaces enclosing the control volume, and the following integral equation is obtained:

$$\frac{d}{ds} \left[\int_A \bar{\rho} \tilde{u} (\tilde{\phi} - \phi_a) dA + \int_A \phi_a (\bar{\rho} \tilde{u} - \rho_a v_a \cos \theta) dA \right] = \oint_{L_p} (\tilde{\phi} \bar{\rho} \tilde{v}_i - \phi_a \rho_a v_{ai}) \cdot n_i dl + \int_A (S_\phi - S_{\phi_a}) dA, \quad (26)$$

where the quantity $\bar{\rho} \tilde{u} \phi_a$ has been added and subtracted in the first two integrals of the left-hand side. In the first integral of the right-hand side, L_p is the perimeter of A , and n_i is a unit vector normal to the center line and to L_p . As discussed in section 4, the ambient magnitudes vary in a characteristic length which is much larger than R_ϕ , so that ϕ_a will be approximately constant over A and can be taken out of the second integral on the left hand side. The first integral in the right hand side represents the entrainment of ambient flow. For this integral to be finite, the radial velocity perturbation, $(\tilde{v}_i - v_{ai}) n_p$ must decay as $1/r$. If it is assumed that Ψ_ϕ decays faster than $1/r$ (otherwise the first integral of equation (26) would not converge), then all the variables can be considered as constant ($\tilde{\phi} \approx \phi_a$) over the perimeter L_p , and can be taken out of the integral. Using equations (21) and (22), equation (26) can be written as

$$\frac{d}{ds} (\dot{m} \langle \tilde{\phi} \rangle) = \phi_a \dot{m}'_0 + \Delta \Sigma_\phi + \dot{m}_a \frac{d\phi_a}{ds}, \quad (27)$$

where

$$\dot{m}'_0 = \frac{d\dot{m}_a}{ds} - \lim_{A \rightarrow \infty} \oint_{L_p} (\bar{\rho} \tilde{v} - \rho_a \vec{v}_a) \cdot \vec{n} dl \quad (28)$$

is the entrained mass per unit length and time, and

$$\Delta \Sigma_\phi = \lim_{A \rightarrow \infty} \int_A (S_\phi - S_{\phi_a}) dA \quad (29)$$

is the source term. Equation (27) applies to the same variables appearing in equation (1); in particular, taking $\tilde{\phi} = 1$, we get $d\dot{m}/ds = \dot{m}'_0$. It should be

noticed that in the integrands of equations (21), (22), (28) and (29) the corresponding ambient values are subtracted, so that the integrals converge as A tends to infinity. In the limiting situation where the effect of the plume is null, all the integrals are zero, and equations (21), (22), (27) and (28) are satisfied identically. The last term of equation (27) is like an additional source representing the effect of the variation of ambient flow properties as we move along the center line. Its effect is very small, and it can be neglected except for large values of s , when $\langle \tilde{\phi} \rangle$ becomes very similar to ϕ_a .

5.3. Mass Entrainment Assumptions

To estimate the mass entrainment, two classical models are used. In the first one,

$$\frac{d\dot{m}}{ds} = \dot{m}'_0 = 2\pi b \rho_a \sqrt{\frac{\rho_m}{\rho_a}} (\alpha |\langle \tilde{u} \rangle - v_a \cos\theta| + \beta |v_a \sin\theta|), \quad (30)$$

where the factor $(\rho_m/\rho_a)^{1/2}$ is due to Ricou and Spalding (1961), and α and β are given the values of 0.057 and 0.5, respectively, in the present work. In the second model, due to Tamanini (1981), the following relation is proposed:

$$\dot{m}'_0 = C_m \mu_{tm}, \quad (31)$$

where the average turbulent viscosity is evaluated using the classical k - ε method directly applied to the average values:

$$\mu_{tm} = C_\mu \rho_m \frac{\langle k \rangle^2}{\langle \varepsilon \rangle}. \quad (32)$$

Equation (31) is based on the analytical solution for a jet (Schlichting, 1968), that for both laminar and turbulent jets gives the value $C_m = 8\pi$, whereas for turbulent jets Ricou and Spalding (1961) give the value $C_m = 5.5\pi$, that is also the value used by Caulfield *et al.* (1993). For laminar plumes Yih (1951) gives the value $C_m = 12\pi$ and Tamanini (1981) takes the value $C_m = 7\pi$. In the present model, $C_m = 6\pi \approx 19$, that, as we will show, is consistent with the Gaussian distribution. Caulfield *et al.* (1993) include an additional term in equation (31) to take into account the transverse component of the wind.

5.4. Relationship between Average Values and Distribution Parameters

If all the turbulent Prandtl numbers for the different variables ϕ are equal, it may be justified that the function Ψ_ϕ and the radius R_ϕ are the same for all the magnitudes, and will be termed Ψ and R , respectively. Then the following relation, obtained from equations (16) and (21) to (25), holds for all ϕ 's:

$$\gamma = \frac{\langle \tilde{\phi} \rangle - \phi_a}{\phi_c - \phi_a} = \frac{R^2}{b^2}, \quad (33)$$

where γ can be obtained from

$$\gamma = \frac{\int_0^\infty (\bar{\rho}\bar{u} - \rho_a v_a \cos\theta) \Psi dA}{\int_0^\infty (\bar{\rho}\bar{u} - \rho_a v_a \cos\theta) dA}. \quad (34)$$

To calculate the density in a cross-section, equations (5), (6) and (8) should be used. However, if radiation and unmixedness were neglected and c_p were constant, the temperature could be obtained directly as a function of the mixture fraction and the following parameters: ξ_s , T_a , T_1 , and the adiabatic flame temperature, T_f . It has been found that using an appropriate lower value of the adiabatic flame temperature, T_f^* , the temperature profiles are almost equal to those obtained when radiation and unmixedness are retained. In Figure 2, the parameter γ for a Gaussian profile and natural gas, obtained using this approximate method, is presented as a function of the mixture fraction at the center line, ξ_c , and for two different values of T_f^* . It can be observed that γ is not very sensitive to the variations of T_f^* . The value of γ tends to 0.5 far downstream, and has a minimum around the tip of the flame, where $\xi_c = \xi_s$.

When the turbulent Prandtl numbers for the variables ϕ are different, there is no reason for the different ψ_ϕ 's to be the same for all ϕ 's, and equations (33) and (34) will only be valid when ϕ is any of the velocity components.

5.5. General Formulation of the Source Term

If the distribution profile ψ_ϕ were a top-hat, the source term defined in equation (29) would be

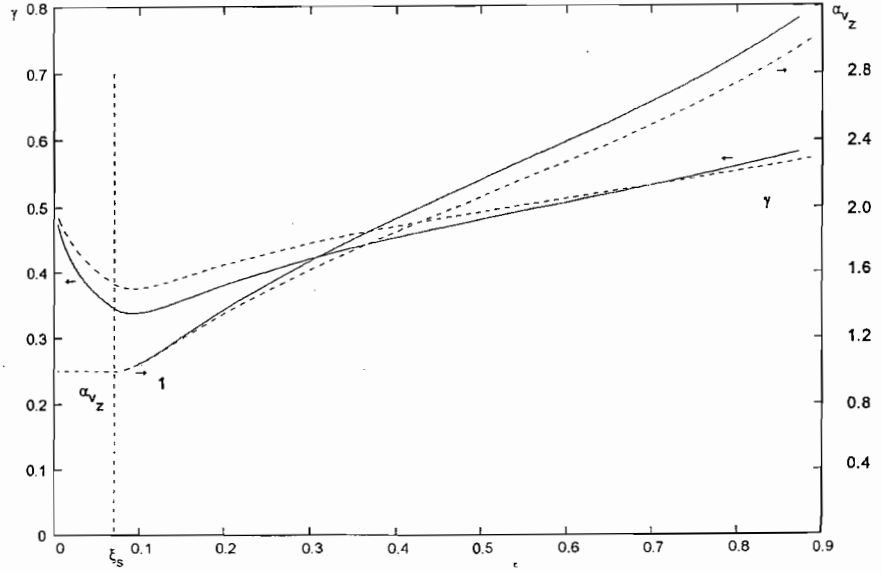


FIGURE 2 Shape parameter γ and coefficient α_{vz} in the source term in momentum equation as functions of ξ_c for two different values of the apparent adiabatic flame temperature. Gaussian profiles. Natural gas. Continuous line: $T_f^*/T_f = 1$; dashed line: $T_f^*/T_f = 0.7$.

$$\Delta\Sigma_\phi = (S_\phi - S_{\phi_a})\pi b^2. \quad (35)$$

For other distributions, it is convenient to write this term in the form

$$\Delta\Sigma_\phi = \alpha_\phi (\hat{S}_\phi - S_{\phi_a})\pi b^2; \quad \hat{S}_\phi = S_\phi(\langle\phi_i\rangle), \quad (36)$$

where \hat{S}_ϕ is defined by substituting the local values of the variables by their averaged values. For a top-hat, α_ϕ would be equal to one. Servvert (1993) has shown that these coefficients mainly depend on the value of the mixture fraction at the center of the jet, ξ_c , and has evaluated them for a Gaussian profile and natural gas flames. Far downstream, ϕ gets close to ϕ_a , the dependence of the integrand of the source term (equation (29)) on $(\phi - \phi_a)$ can be linearized, and it can be shown that α_ϕ tends to one. The α_ϕ coefficients have been calculated with the same procedure used to obtain the values of γ presented in Figure 2; it has also been found that they do not depend very much on T_f^* .

5.5.1. Source Term in the Momentum Equation

In the vertical momentum equation, the buoyancy term is

$$\Delta\Sigma_{vz} = \lim_{A \rightarrow \infty} \int_A (\rho_a - \bar{\rho}) g_r dA = \alpha_{vz} (\rho_a - \rho_m) \dot{g}_r \pi b^2, \quad (37)$$

where g_r represents the gravity acceleration. The coefficient α_{vz} is larger than one upstream of the flame tip; its variation as a function of the mixture fraction in the center line of the jet, for natural gas, is shown in Figure 2.

5.5.2. Source Term in the Energy Equation

If the gas is optically thin and the absorption coefficient is constant in the plane normal to the center line, equation (36) can be written as follows:

$$\Delta\Sigma_h = -\alpha_h \varepsilon_r \sigma_b (\langle \tilde{T} \rangle^4 - T_a^4) 2\pi b, \quad (38)$$

where σ_b is the Stefan-Boltzmann constant and $\varepsilon_r = 2ba$, with a being the absorption coefficient. This equation has been generalized to the case of a non-thin gas, assuming that the flame is locally a cylindrical surface of radius b and emissivity ε_r . The factor α_h accounts for the temperature variation inside the flame. The variation of α_h with mixture fraction in the center line, for natural gas, is shown in Figure 3. It is much larger than one in the rich region upstream of the flame. An alternative approach is used in Hernández *et al.* (1995), where the radiative losses are assumed to be a fixed fraction of the heat of reaction; the results using this approach and the one proposed here are compared in Section 6. The method proposed by Modak (1979) is used to evaluate ε_r from the mass fractions of CO_2 , H_2O and soot. The emissivity of the mixture of soot and gas is expressed by: $\varepsilon_r = \varepsilon_s + \varepsilon_g - \varepsilon_s \varepsilon_g$; the soot emissivity, ε_s , is obtained as a function of soot concentration, temperature and plume radius, b , combined as an argument of the pentagamma function; the gas emissivity is obtained from: $\varepsilon_g = \varepsilon_c + \varepsilon_w - \Delta\varepsilon_{cw}$, where the emissivities of CO_2 , ε_c , and of H_2O , ε_w , are obtained from expressions involving the Chebyshev polynomials, whose arguments depend on the partial pressure of each component, temperature, and radius b . The overlap correction $\Delta\varepsilon_{cw}$ is also given as a function of the previous parameters.

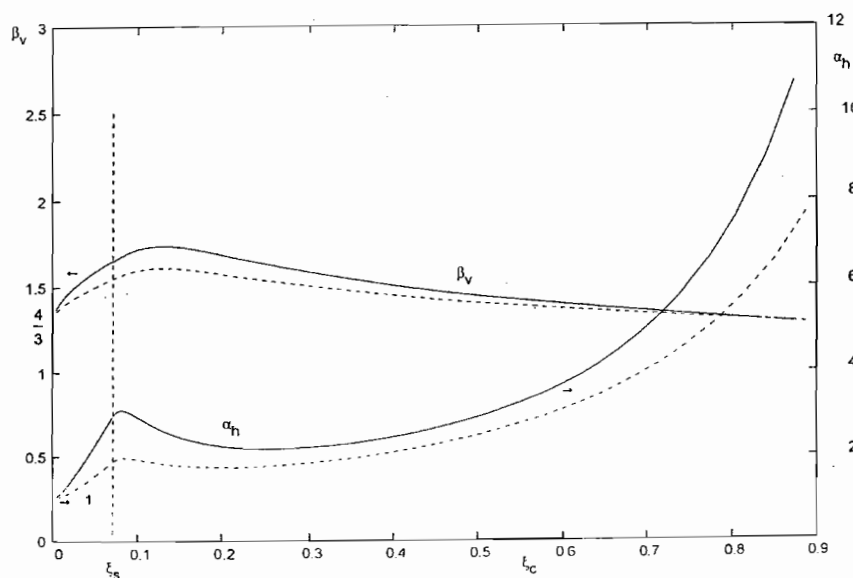


FIGURE 3 Coefficient α_h in the source term in the energy equation, and shape parameter for the velocity modulus, β_v , that appears in the equation for the production of k , as functions of ξ_c , and for two different values of the apparent adiabatic flame temperature. β_v corresponds to the case of large values of the jet velocity compared to the ambient velocity. Gaussian profiles. Natural gas. Continuous line: $T^*/T_f = 1$; dashed line: $T^*/T_f = 0.7$.

5.5.3. Source Terms in the Turbulent Kinetic Energy Equation

For the turbulent kinetic energy, there are three source terms. The mechanical production term, $\Delta\Sigma_{k1}$, could be estimated using a direct calculation (Caulfield *et al.*, 1993),

$$\Delta\Sigma_{k1} = \mu_{tm} \lim_{A \rightarrow \infty} \int_A \left(\frac{\partial(\tilde{u} - v_a \cos\theta)}{\partial r} \right)^2 2\pi r dr, \quad (39)$$

where the parabolic approximation is used. However, this method fails for a top-hat profile, as the integral in equation (39) will diverge. Moreover, it is not expected that equation (39) would be correct for cases in which the velocity gradients of the ambient flow are comparable to those of the perturbed flow. Also, if there is a strong cross wind, when $\theta > 0$, with vortices shed at the back of the jet, there will be additional turbulence created that will not be contem-

plated by equation (39). We have extended an alternative procedure originally suggested by Tamanini (1981) for no-wind and top-hat profiles, to the case of having a cross-wind and any distribution profile in the following manner. From the inner product of the vector momentum conservation equation (1) and the velocity, the conservation equation of mechanical energy is obtained,

$$\frac{\partial}{\partial x_i} \left(\bar{\rho} v_i \frac{\tilde{v}^2}{2} - \tau_{ij} \tilde{v}_j \right) = -S_{k1} - (\bar{\rho} - \rho_a) g_r \tilde{v}_z, \quad (40)$$

where the pressure term has been assumed to be only due to ambient pressure, according to the parabolic approximation, and is included in the buoyancy term. The term S_{k1} , that in this equation appears as a sink term for the kinetic energy of the mean turbulent flow, is also the classical source term in the equation for k ,

$$S_{k1} = \tau_{ij} \frac{\partial \tilde{v}_j}{\partial x_i}. \quad (41)$$

Equation (39) has the same form of equation (1), and taking $\tilde{v}^2/2$ as the magnitude $\tilde{\phi}$, equation (27) can be used to obtain a conservation equation for $\langle \tilde{v}^2/2 \rangle$. In this equation, there will appear two source terms: one of them will be $-\Delta \Sigma_{k1}$, corresponding to $-S_{k1}$ of equation (40), and the other one is due to buoyancy. An equation for $\langle \tilde{v} \rangle^2/2$ can be obtained from the inner product $\langle \tilde{v}_i \rangle d \langle \tilde{v}_i \rangle / ds$, applying equation (27) to each velocity component. By subtracting the conservation equation for $\langle \tilde{v} \rangle^2/2$, multiplied by a factor β_v , from that for $\langle \tilde{v}^2 \rangle/2$, the following expression can be obtained for $\Delta \Sigma_{k1}$,

$$\begin{aligned} \Delta \Sigma_{k1} = & \underbrace{-\dot{m} \frac{1}{2} [\langle \tilde{v} \rangle^2 - v_a^2]}_I \frac{d\beta_v}{ds} + \underbrace{\dot{m}'_0 \frac{1}{2} (\langle \tilde{v} \rangle - \bar{v}_a)^2 \beta_v}_II \\ & + \underbrace{(\rho_a - \rho_m) \langle \tilde{v}_z \rangle g_r (\beta_v \alpha_{vz} - \alpha') \pi b^2}_III \\ & + \underbrace{\left[\beta_v \left[\dot{m} \frac{dv_a^2/2}{ds} - \dot{m}_a \frac{d\bar{v}_a}{ds} \langle \tilde{v} \rangle \right] + \frac{1}{2} \frac{dv_a^2}{ds} (\dot{m}_a - \dot{m}) \right]}_IV, \quad (42) \end{aligned}$$

where α_{vz} has been introduced in equation (37) and given in Figure 2, and the coefficients β_v and α' are defined by the equations

$$\beta_v = \frac{\langle \tilde{v}^2 \rangle - v_a^2}{\langle \tilde{v} \rangle^2 - v_a^2} \quad (43)$$

$$\alpha' = \frac{\lim_{A \rightarrow \infty} \int_A (\rho_a - \bar{\rho}) g_r \tilde{v}_z dA}{(\rho_a - \langle \bar{\rho} \rangle) g_r \langle \tilde{v}_z \rangle \pi b^2} \quad (44)$$

Servet (1993) has shown that α' is equal to one for Gaussian profiles and very approximately equal to one for other profiles. The value of β_v has been calculated similarly to those of γ and α_ϕ , and assuming that the jet velocity, \tilde{v} , is always much larger than the ambient velocity, v_a . This parameter is presented in Figure 3; it can be observed that it reaches a maximum around the position where $\xi_c = \xi_s$, and, as ξ_c tends to zero, it tends to 4/3. However, as ξ_c tends to infinity β_v should tend to one. Then, there should be a downstream transition region, not represented in Figure 3, where ξ_c is very small, the velocity $\langle \tilde{v} \rangle$ changes from a value much larger than v_a to v_a , and β_v changes from 4/3 to 1.

In Figure 4 are presented, for a typical case, the values of the contributions indicated in equation (42); contribution IV is so small that can not almost be discerned with the scale used. The most important term is II, which is analogous to the expression proposed by Tamanini (1981), generalized to profiles different from a top-hat with cross wind; it expresses that the turbulent kinetic energy is created inside the plume at a rate determined by the kinetic energy of the relative velocity of the entrained flow. A maximum of term II is reached at around the position of the flame tip, where $\xi_c = \xi_s$. Upstream of this maximum, term II increases mainly because of the increase in temperature and decrease of the density that dilates the gas and makes both the jet diameter and the entrainment rate larger.

Term I (including the minus sign) is associated to the variation of β_v ; this term is positive downstream of a section near the flame tip, where $d\beta_v/d\xi_c > 0$ (see Fig. 3 and note that $d\xi_c/ds < 0$), and negative upstream. The absolute value of term I is everywhere much smaller than term II, except close to the exit, where ξ_c is of order unity, and in a short region downstream from the flame tip. This behavior can be checked as follows: from equation (27) applied to $\phi = \xi$, it is deduced that $d\langle \tilde{\xi} \rangle/ds = -(\dot{m}'_0/\dot{m})\langle \xi \rangle$, and, consequently, $d\beta_v/ds = -(d\beta_v/d\langle \tilde{\xi} \rangle)(\dot{m}'_0/\dot{m})\langle \xi \rangle$; then, the ratio between terms I and II is (I)/(II) $\sim \langle \tilde{\xi} \rangle$

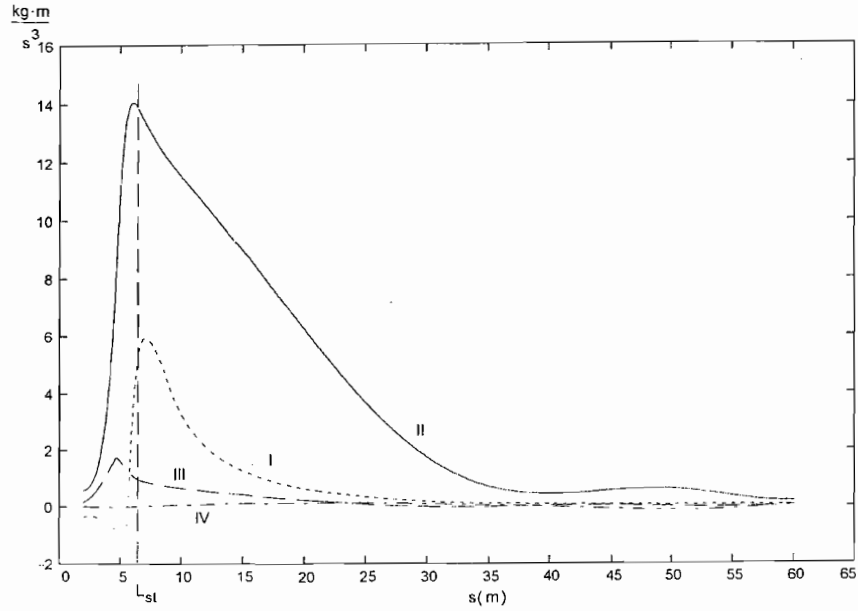


FIGURE 4 Comparison of the different terms that contribute to the mechanical production of turbulent kinetic energy. Horizontal flame. $Fr = 20000$, $D = 10$ cm, $v_{oH}/u_1 = 0.1$.

$(d\beta_v/d\langle\tilde{\xi}\rangle)$, and, on using the equality $\langle\tilde{\xi}\rangle = \gamma\xi_c$, this ratio becomes (I)/(II) $\sim \xi_c \gamma (d\beta_v/d\xi_c) / (\gamma + \xi_c d\gamma/d\xi_c)$, that is small whenever ξ_c is small, except close to the tip of the flame on the lean side, where both derivatives, $d\beta_v/d\xi_c$ and $d\gamma/d\xi_c$, are large, of the order of $1/\xi_s$ (see Figs. 2 and 3).

Term III is always positive because both β_v and α_{vz} are larger than one and α' is equal to one. It is associated to the excess of mechanical energy created by buoyancy (as expressed in equation (40)) that does not contribute to the average kinetic energy of the jet; for top-hat profiles, or in the downstream region where $\beta_v = \alpha_{vz} = \alpha' = 1$, this term vanishes. This term should be most important near the flame tip, where the density is lowest. When compared with term II, its relative order of magnitude may be estimated as follows: if we take $\dot{m}'_0 \sim \dot{m}/L_{st}$, where L_{st} is the flame length, and all the densities and velocities are supposed to be of a similar order of magnitude, the ratio of the two terms is (III)/(II) $\sim (g_r L_{st} \sin(\theta)) / \langle\tilde{v}\rangle^2$. On the other hand, from Hernández *et al.* (1995), $L_{st}/D \sim 10.3 Fr^{0.2}$, where D is the exit diameter and $Fr = u_1^2/(g_r D)$ is the Froude number based on the exit velocity, and, from Schlichting (1968), assuming a jet-like behavior, $\langle\tilde{v}\rangle/u_1 \sim 0.14(L_{st}/D)$, so that the ratio of the two terms is

(III)/(II) $\sim 20 \sin(\theta)/Fr^{0.4}$. The relative importance of term III is largest for small Fr and vertical flames.

Term IV is associated to the variation of ambient properties with height and is more important far downstream, where the plume properties are close to their ambient values. There, the values of β_v and of all α 's are close to one, and equation (42) can be rewritten as

$$\Delta \Sigma_{k1} = \underbrace{\dot{m}'_0 \frac{1}{2} (\langle \tilde{v} \rangle - \tilde{v}_a)^2}_{II} + \underbrace{\dot{m}_a \frac{dv_a}{ds} (v_a - \langle \tilde{v}_x \rangle)}_{IV} \quad (45)$$

Term IV may be negative, and can be interpreted as follows: The last term on the right hand side of equation (27) is a production term due to variation of ambient properties. If we examine the equation of conservation of mean mechanical energy, we have a production term $m_a d(v_a^2/2)/ds$. On the other hand, in the equation of conservation of horizontal momentum, the production term $m_a d(v_a)/ds$ is like a force, that multiplied by the horizontal velocity $\langle \tilde{v}_x \rangle$ gives a power. When $\langle \tilde{v}_x \rangle$ is larger than v_a , the power produced by the force is larger than the production of kinetic energy of the mean flow, and the difference is expected to be extracted from the turbulent kinetic energy. The relative importance of this term may be estimated as follows: the entrainment should behave like the ambient viscosity, $\dot{m}'_0 \sim \rho_a u^* z$, and the variation of velocity goes like $dv_a/ds \sim dv_a/dz \sin(\theta) \sim u^*/z \sin(\theta)$; then, the relative importance of both terms is (IV)/(II) $\sim (b/z)^2 \sin(\theta) [v_a/(\langle \tilde{v}_x \rangle - v_a)]$. As the plume reaches ambient conditions, it is to be presumed that $(\langle \tilde{v}_x \rangle - v_a) \sim \langle \tilde{v}_y \rangle \sim v_a \sin(\theta)$, so that (IV)/(II) $\sim (b/z)^2$, and, as the plume height is much larger than the radius, the relative importance of term IV is always small.

The entrainment rate \dot{m}'_0 can be obtained by eliminating $\Delta \Sigma_{k1}$ between equations (39) and (42). For a self-similar jet without lateral wind and neglecting buoyancy, only term II of equation (42) is non-zero. Using the profile defined in equation (19), the definition given in equation (21), and assuming incompressible flow, $\langle \tilde{v}^2 \rangle$ and $\langle \tilde{v} \rangle$ can be calculated; then, on using equation (43), β_v is obtained. If it is assumed that μ_t is constant in a cross-section, it is obtained from equations (39) and (42) than \dot{m}'_0 has to be of the form given by equation (31) and the coefficient C_m has the value 8π , in agreement with Schlichting's (1968) solution for a jet. If we choose the Gaussian profile (equation (18)), $C_m = 6\pi$, and for a cosine-type profile (equation (20)), $C_m = 6.06\pi$. Under the previous restrictive conditions, the two

methods, based on equations (39) and (42), to calculate $\Delta\Sigma_{k1}$ will give the same result if equation (31) is used to calculate the entrainment, and the appropriate value of C_m is chosen. It is of interest to know what happens in the general case of a compressible non-axisymmetric flame. In Figure 5, the values of $\Delta\Sigma_{k1}$ obtained using equations (39) and (42) are compared, for a typical case, and the differences are reasonably small, except near and downstream of the cross-section where the flame tip is located, where term I of equation (42), associated to the variation of β_v , is largest. The level of difficulty associated to the application of the two equations is similar: the integral of equation (39) is quite straightforward, and can even be performed analytically. The main advantage of equation (42) is that it is of a more general validity, and can be applied more confidently when the shape of the profile, $\psi(r/R)$, is not well known, because it is less sensible to its choice which is taken into account in equation (42) through the factor β_v . This factor may only change from 1, for a top-hat or when the velocity is close to the ambient one, to a maximum of 1.6, in a Gaussian profile near the flame tip (Fig. 3), whereas the integral of equation (39) experiences much larger changes with the shape of the profile and even tends to infinity as a top-hat profile is approached.

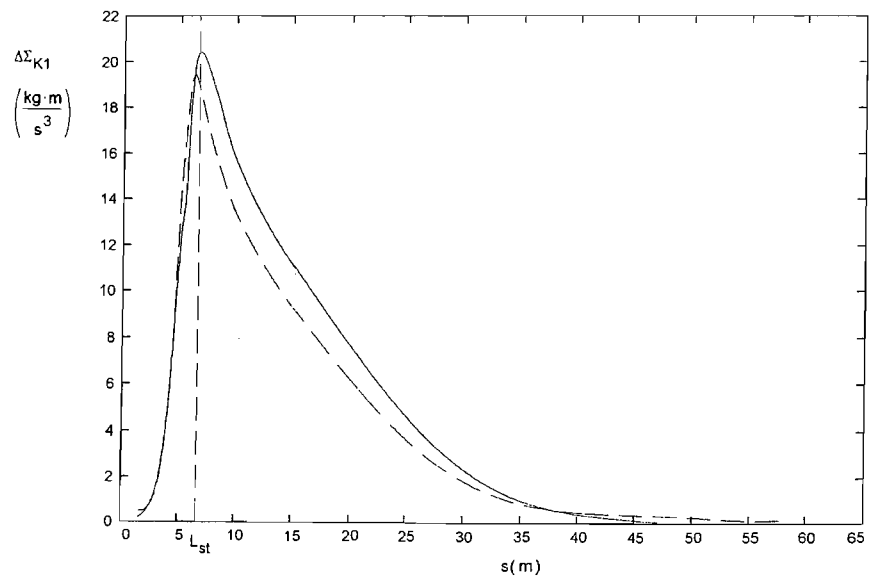


FIGURE 5 Comparison of the mechanical production of turbulent kinetic energy obtained using equation (39) (dashed line) and (42) (solid line). Horizontal flame. $Fr = 20000$, $D = 10$ cm, $v_{aH}/u_1 = 0.1$.

The production of $\langle k \rangle$ by buoyancy is given by

$$\Delta \Sigma_{k2} = \alpha_{k2} \frac{g_r}{\sigma_h} \left(\frac{\langle \tilde{\mu} \rangle d\langle \bar{\rho} \rangle}{\langle \bar{\rho} \rangle ds} - \frac{\mu_a d\rho_a}{\rho_a ds} \right) \pi b^2 \sin\theta. \quad (46)$$

Using arguments similar to those applied to estimate the order of magnitude of term III in equation (42), it can be shown that this term, when compared with term II of equation (42), is even smaller than term III, of an order $\Delta \Sigma_{k2}/(\text{II}) \sim \sin\theta/\text{Fr}^{0.8}$, and, in practical cases, is always negligible.

For the dissipation rate of $\langle k \rangle$,

$$\Delta \Sigma_{k3} = -\alpha_{k3} (\langle \bar{\rho} \rangle \langle \varepsilon \rangle - \rho_a \varepsilon_a) \pi b^2, \quad (47)$$

where, as it has been shown by Servvert (1993), the coefficient α_{k3} is also close to one.

5.5.4. Source Terms in the Equation for the Dissipation Rate of the Turbulent Kinetic Energy

We consider that the source terms in equation for $\langle \varepsilon \rangle$ are equal to those in equation for $\langle k \rangle$ corrected by the factor $\langle \varepsilon \rangle / \langle k \rangle$ and affected by the classical constants of the k - ε model: $C_{\varepsilon 1} = 1.44$, $C_{\varepsilon 3} = 0.95$, and $C_{\varepsilon 2} = 1.92$, for the three terms appearing respectively in equations (45) to (47).

5.5.5. Source Terms in the Equation for the Variance of the Mixture Fraction

The production of g is given by

$$S_{g1} = \frac{2}{\sigma_\xi} \mu_t (\nabla \tilde{\xi})^2 \quad (48)$$

Proceeding in the same manner as for the k production term $\Delta \Sigma_{k1}$ of equation (42), the following relation is obtained

$$\Delta \Sigma_{g1} = -\frac{d\beta_\xi}{ds} \dot{m} \langle \tilde{\xi} \rangle^2 + \beta_\xi \dot{m}'_0 \langle \tilde{\xi} \rangle^2, \quad (49)$$

where the coefficient β_ξ is analogous to β_v defined in equation (43),

$$\beta_\xi = \frac{\langle \tilde{\xi}^2 \rangle}{\langle \tilde{\xi} \rangle^2}. \quad (50)$$

The two terms of equation (49) are similar to terms I and II, respectively, of equation (42), and similar comments can be made.

The dissipation term in the three-dimensional equation for g is used in the one-dimensional equation by direct substitution of the averaged quantities, and the correction coefficient is considered equal to one, so that

$$\Delta \Sigma_{g2} = -C_g \rho_m \langle \varepsilon \rangle \frac{\langle g \rangle}{\langle k \rangle} \pi b^2, \quad (51)$$

where $C_g = 0.8$ is a constant of the k - ε - g model.

5.6. Exit Conditions

At the exit mouth it is assumed that the conditions are known and have a top-hat distribution. There is a short initial transition region, of the order of five to ten diameters, in which the profiles are chosen as a linear combination of top-hat and Gaussian ones, and where the additional condition that the maximum value of $\tilde{\phi}$ is equal to that at the exit is imposed. This assumption is not valid for g and ε , which are expected to be largest at the borders of the jet, and consequently will not be even qualitatively described by a linear combination of a top-hat and a Gaussian profile. However, beyond the short transition region, the profiles of all the variables, even those of g and ε , behave similarly to Gaussian ones.

For the exit values of k and ε , we have taken $k_1 = \lambda v_1^2 / 8 C_\mu^{0.5}$ and $\varepsilon_1 = 2k_1^{3/2} / D$ (Hernández *et al.*, 1995), where D is the pipe diameter and λ is the classical head loss factor taken from Moody's diagram, corresponding to the discharging pipe. Nevertheless, turbulence properties at the exit are found to have negligible influence on flame evolution.

When the stagnation pressure of the exit gas is high enough, choking conditions are reached at the exit. To calculate the expanded conditions, that are the equivalent exit conditions, we use an approach similar to that proposed by Birch *et al.* (1987), except that the stagnation enthalpy, instead of temperature, is assumed to be constant in the expansion.

The lift-off effect has been incorporated into the model considering that the combustion process is inhibited until a certain distance, which is determined according to the correlations proposed in Crespo *et al.* (1994).

6. COMPARISON WITH EXPERIMENTS AND RESULTS OF THE 3D MODEL

Verheij and Duijm (1991) carried out experiments in which they measured temperature distributions in the middle vertical section of a flame, corresponding to a release of natural gas through a 5 mm nozzle at a height $H = 250$ mm over the ground, for different fuel exit velocities and wind speeds. The ground roughness was $z_0 = 3.8 \times 10^{-5}$ m. Hernández *et al.* (1995) show that several effects such as the choice of different probability density function for the mixture fraction (that is required in the $k-\epsilon-g$ model), or the influence of ambient turbulence are small, so that the only relevant non dimensional parameters appearing in the problem are the Froude number based on exit conditions, $Fr = u_1^2/(gD)$, and the ratio of ambient velocity at the height of the exit pipe to the fuel velocity at the exit, v_{aH}/u_1 . In Crespo *et al.* (1994) five cases are presented, and for each one of them the results of the full 3D elliptic model, of a parabolic version of it, and of the 1D model are compared with those of the experiments. In this work, we present in Figure 6 only the case corresponding to $Fr = 14009$ and $v_{aH}/u_1 = 0.029$ that is considered to be representative, and compare the results of the 1D model with those of the elliptic 3D model and experimental measurements. The agreement is good, although the temperature contours are in general longer and thinner in the one-dimensional model than in the three-dimensional one; in general, there seems to be a better agreement of experiments with the 3D elliptic code than with the 1D code. As it will be discussed later, this discrepancy may be due to the fact that the Prandtl number used by Hernández *et al.* (1995) is $\sigma_\xi = 0.7$, whereas in the 1D model proposed here, $\sigma_\xi = 1.0$.

In Figures 7a and 7b, a comparison is made between the temperature distribution in a cross-section calculated with the 1D model and measurements described in Bennett *et al.* (1991); these measurements correspond to a release of pressurized natural gas, so that it is necessary to calculate the expanded conditions to apply the 1D model, as indicated in Crespo *et al.* (1994). In these figures are also presented the rescaled results of a small-scale experiment, made by Bakkum (1994) at the scale 1/35, maintaining Froude number similarity, and using as initial velocity and diameter those corresponding to the expanded jet. The large-scale release corresponds to a mass flow rate of natural gas of 8.6 kg/s, an exit diameter of 152 mm, a wind velocity of 0.2 m/s, a burner height of

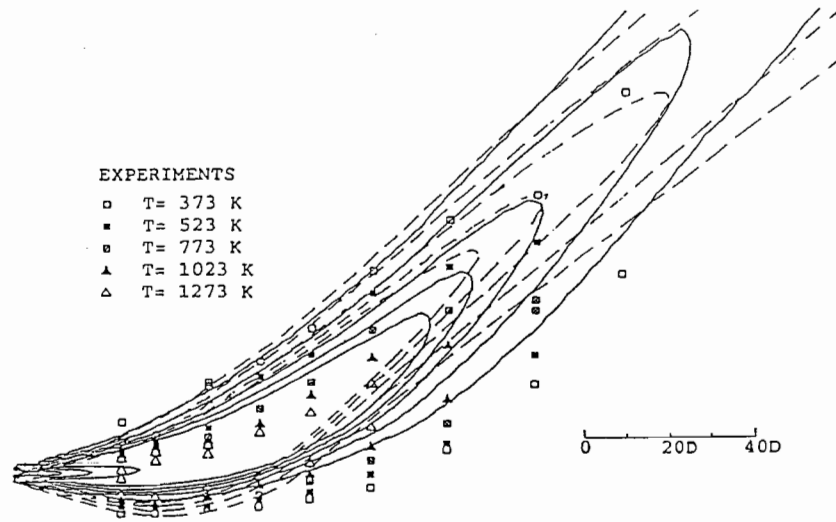


FIGURE 6 Comparison of temperature contours obtained with the 3D elliptic code and the 1D code. $Fr = 14,009$, $v_{aH}/u_1 = 0.029$. Continuous line: elliptic code; dashed line: 1D code.

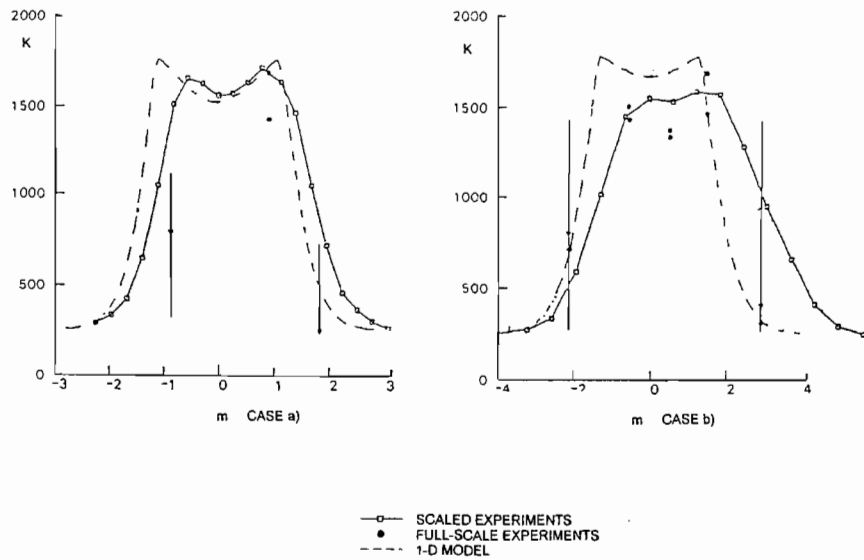


FIGURE 7 Comparison of temperature distributions at different cross sections, calculated with UPMFIRE, with both large (Bennet *et al.*, 1991) and small scale (Bakkum, 1994), experiments, that are supposed to be similar. Case a) downwind distance: 7 m. Case b) downwind distance: 12 m.

3 m, and a surface roughness of 1 cm. The cross sections of Figures 7a and 7b are at a height of 3.5 m above the ground, at downwind distances from the exit of 7 and 12 m, respectively. The temperatures measured in the field tests exhibit variations due to meandering effects, and the plotted data, indicated by black dots, are averaged values; vertical bars are drawn to indicate the lowest and highest observed temperature values at locations where large fluctuations and intermittency were observed. The results from the small-scale tests are indicated by a solid line, and those of the 1D model by a dashed line. In the profiles predicted by the 1D model there are two maxima and a minimum indicating that the cross-section is upstream of the flame tip; this can also be observed for the wind-tunnel experiments in Figure 7a, but not so clearly in Figure 7b, what means that the flame length predicted by the 1D model is slightly longer than the one measured in wind tunnel. However, for both figures the agreement with wind-tunnel measurements is good, and better for the upstream section (Fig. 7a). The agreement with full scale experiments is also good, but in this case is better for the downstream section (Fig. 7b). The peak temperatures predicted by the 1D model are larger than the measured ones, both in large-scale and wind-tunnel experiments.

In Hernández *et al.* (1995), the geometric characteristics of the flame surface, defined as the surface where the average mixture fraction has its stoichiometric value, have been calculated using the 3D elliptic code. These overall characteristics in non-dimensional form turn out to be mainly functions of Fr and v_{aH}/u_1 . In particular, for horizontal flames, the non-dimensional flame length, L_{st}/D , increases with both v_{aH}/u_1 and Fr , and the following correlation has been proposed (Crespo and Hernández, 1993) to describe this behavior:

$$\frac{L_{st}}{D} = 10.3 \left(1 - 3.5 \frac{v_{aH}}{u_1} \right) Fr^{(0.2 + 0.9 v_{aH}/u_1)}, \quad (52)$$

for $1000 < Fr < 15000$ and $0 < v_{aH}/u_1 < 0.1$. This correlation is identical to another one proposed by Ott (1993), based on measurements of visible flame lengths, if the stoichiometric to visible flame length ratio is 0.61, which is within the range of variation of this ratio predicted by other authors, and $v_{aH}/u_1 = 0$, as discussed in Hernández *et al.* (1995). In Hernández *et al.* (1995) is also compared the ratio L_{st}/D predicted by the 3D elliptic code with the results of another 1D model proposed by Peters and Göttgens (1991), and a very good agreement is found. The calculations of Hernández *et al.* (1995) were carried out using a value of $\sigma_\xi = 0.7$, and Peters and Göttgens (1991) took $\sigma_\xi = 0.71$. In the 1D model presented here it has been assumed that $\sigma_\xi = 1.0$, so that in order

to compare with the results of Hernández *et al.* (1995) and Peters and Göttgens (1991) it is necessary to account for the influence of σ_ξ . The influence of σ_ξ could be approximately taken into account by considering that the transverse profile is $\Psi_\xi = \exp(-\sigma_\xi(r/R)^2)$, instead of equation (18); then, on using equations (21) and (22) and assuming constant density, it can be shown that the ratio of the maximum and average values of the mixture fraction, $\xi_c/\langle\xi\rangle$, is $(1 + \sigma_\xi)$, instead of the value 2 predicted by equations (33) and (34). However, near the flame, density variation is important, and, as it is associated to the variation of temperature and, consequently, of mixture fraction, a larger influence of σ_ξ on ξ_c is expected. Peters and Göttgens (1991) take into account density variations by using a mass weighted similarity variable and assuming that the Chapman-Rubesin parameter is constant, and find that ξ_c is proportional to $(1 + 2\sigma_\xi)/3$. However, the results that are shown next indicate that the influence of σ_ξ is even larger, and that ξ_c should be proportional to σ_ξ . For horizontal flames that are mainly momentum dominated, the mass fraction is expected to decrease as $1/s$, so that the flame length, L_{st} , defined as the value of s where $\xi_c = \xi_{st}$, should also be proportional to ξ_c and should be multiplied by the factor affecting ξ_c . The best agreement between the 1D calculations and those of Hernández *et al.* (1995) is obtained if this factor is σ_ξ . This correction has been included in the results of the 1D calculations shown in Figure 8 for horizontal flames. For this figure, the exit height is $H = 2$ m and the surface roughness is $z_0 = 0.5$ mm, so that the ambient turbulence is $1/\ln(H/z_0) = 0.11$; Hernández *et al.* (1995) have shown that the influence of the ambient turbulence is small. The exit velocity and diameter are changed in the ranges: $v_1 = 10$ to 150 m/s, and $D = 0.5$ to 5 cm, respectively; this means that, besides Fr and v_{aH}/u_1 , two other non-dimensional parameters are changed: H/D and the ratio of radiative losses to heat of combustion. The results of Figure 8 show that the main dependence is with Fr and v_{aH}/u_1 , because all the calculated points with the same value of v_{aH}/u_1 fall very approximately on the same curve. Also, in Figure 8, a comparison is made with the results of equation (52) in the appropriate range, and with numerical results of Hernández *et al.* (1995) for Fr = 100,000, and a good agreement is found, although for low values of Fr the flame lengths are slightly overpredicted by the 1D model, and for Fr = 100,000 and $v_{aH}/u_1 = 0$ are slightly underpredicted. Figure 8 also includes results of small scale experiments (Bakkum, 1994). It has been supposed that the flame lengths reported by Bakkum (1994) are visible, so that the same previous factor 0.61 has been applied to transform them to stoichiometric flame lengths. The agreement between the results of experiments and those of the 1D code is acceptable.

Figure 9 corresponds to vertical flames; the range of variation of the parameters is as in Figure 8. In this case, the influence of σ_ξ is smaller, because

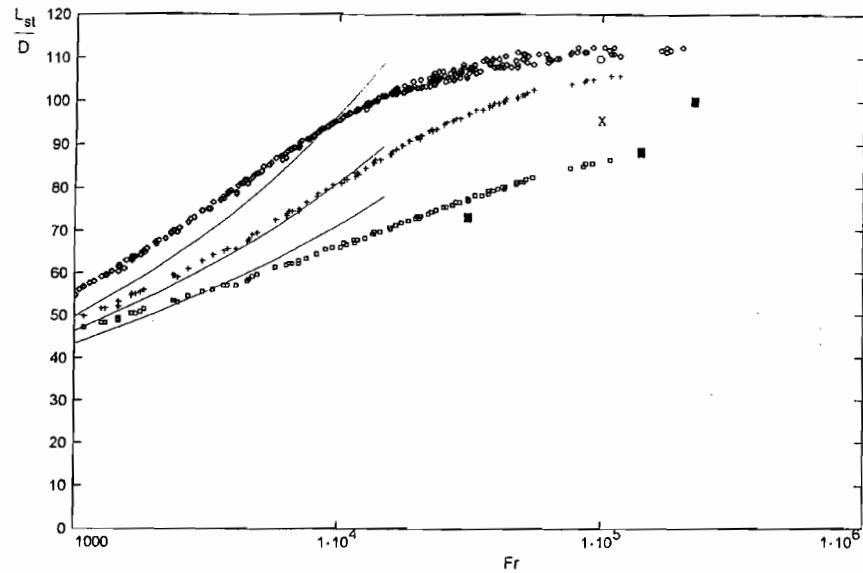


FIGURE 8 Comparison of non-dimensional horizontal-flame lengths calculated with the 1D model, correlation (52), affected by the factor $\sigma_z = 0.71$, and with the 3D elliptic code, and experimental results of Bakkum (1994). Continuous line: correlation of Crespo and Hernández (1993), equation (52). \square 1D model, $v_{aH}/u_1 = 0$. \diamond 1D model, $v_{aH}/u_1 = 0.05$. \circ 1D model, $v_{aH}/u_1 = 0.10$. \circ Hernández *et al.* (1995) for $Fr = 100,000$ and $v_{aH}/u_1 = 0.10$. \times Hernández *et al.* (1995) for $Fr = 100,000$ and $v_{aH}/u_1 = 0$. \blacksquare experiments of Bakkum (1994) $v_{aH}/u_1 = 0$.

for buoyancy-dominated flames the mixture fraction decays more slowly with distance, like $1/s^{2/5}$, and if the same criterium as above is used, the factor should be $\sigma_z^{2/5} = 0.87$. However, this factor gives flames slightly shorter than those calculated by Hernández *et al.* (1995), and a much better agreement is obtained if the factor is deduced from the criterium of constant density indicated above: $[(1 + \sigma_z)/2]^{2/5} = 0.94$. In Figure 9 a comparison is made of the 1D results affected by that factor with a correlation of Becker and Liang (1978) that is in excellent agreement with the results of Hernández *et al.* (1995) for $v_{aH}/u_1 = 0$. However, as v_{aH}/u_1 increases, the flame length predicted by the 1D model increase, instead of decreasing as predicted by Hernández *et al.* (1995). These authors also predict that for a certain value of v_{aH}/u_1 , that depends on Fr , the flame length reaches a minimum, and for further increases of v_{aH}/u_1 , the flame length starts to increase again. This discrepancy may be interpreted as though the minimum, that in Hernández *et al.* (1995) appeared for v_{aH}/u_1 in the range 0.05 to 0.15, now appears around $v_{aH}/u_1 = 0$. Since the

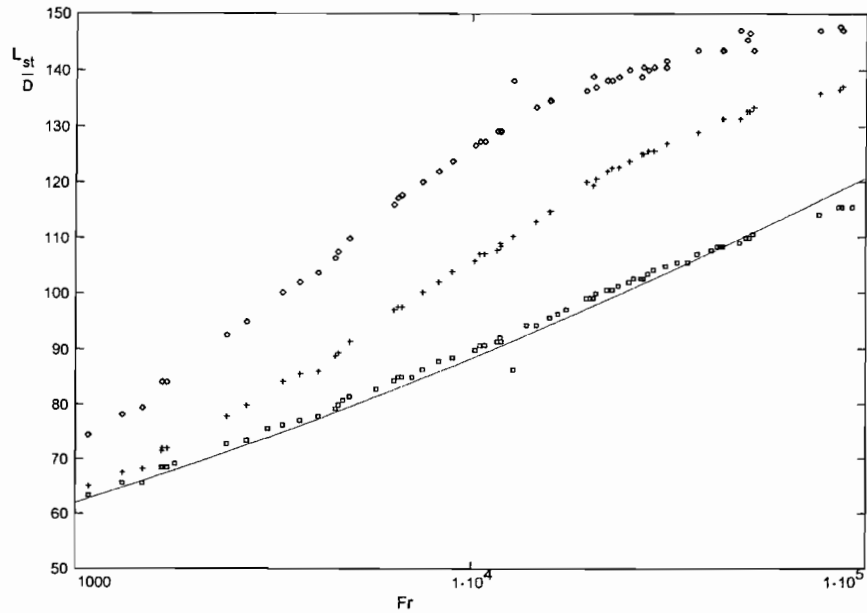


FIGURE 9 Non-dimensional vertical-flame lengths calculated with 1D model, affected by the factor $[(1 + \sigma_s)/2]^{2/5} = 0.94$; \square $v_{aH}/u_1 = 0$; $+$ $v_{aH}/u_1 = 0.05$; \diamond $v_{aH}/u_1 = 0.10$. Comparison with correlation of Becker and Liang (1978) for $v_{aH}/u_1 = 0$ (continuous line) that agrees well with the calculations of Hernández *et al.* (1995).

1D model is derived from the 3D equations assuming that the flow is parabolic along the center-line of the flame, it is to be expected that for the case that the flame is vertical and there is no lateral wind, this assumption will hold better than when there is lateral wind and $v_{aH}/u_1 \neq 0$.

Although, as it has been seen, the influence of radiation on flame length is small, it is also of interest to estimate its influence on temperature distribution. Hernández *et al.* (1995) assumed that the radiative losses were a fixed fraction, 19%, of the heat of reaction and accordingly used a correlation proposed by Sivathanu and Faeth (1990) for $T(\xi)$. In Figure 10 are compared the average temperature distributions, $\langle T \rangle$, using expression (38) for the radiative losses, assuming that they are a fixed fraction of the heat of reaction, and without radiation losses, for two values of Fr. Upstream of the flame, the temperatures calculated with the 1D model are somewhat larger, and downstream smaller than those obtained assuming that the radiative losses are a fixed fraction of the heat of reaction.

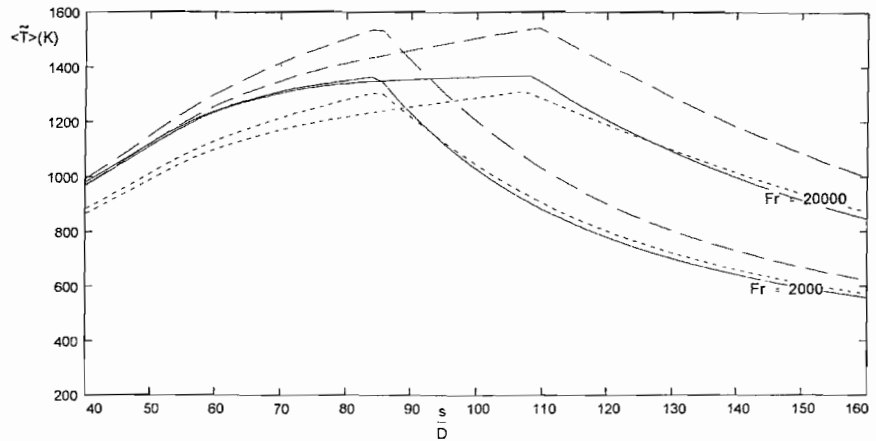


FIGURE 10 Comparison of the average temperature, $\langle T \rangle$, distribution along the flame, calculated with heat losses as in equation (38) (continuous line) as a fixed fraction of the heat of reaction (short dashed line) and with no radiation losses (long dashed line) for two values of $Fr = 2000$ and 20000 . Horizontal flame. $v_{aH}/u_1 = 0.0$.

7. CONCLUSIONS

A procedure has been presented to obtain a one-dimensional (1D) model of turbulent jet diffusion flames for releases of gaseous fuels in the presence of a non-uniform incident wind. The model is deduced from a parabolic three-dimensional (3D) formulation of the fluid dynamics equations complemented with models for chemical reaction, thermal radiation and an adaptation of the k - ϵ - g closure method. Self-similar profiles in planes normal to the center line are assumed, that can extend radially to infinity. New terms, not present in the literature, appear in the 1D conservation equations as a consequence of the variation of the ambient properties with height. An alternative procedure for the production of the turbulent kinetic energy and of the mixture fraction variance, that is less dependent on the choice of the transverse profile, is proposed. Results obtained with the model have been compared with those of the three-dimensional model, developed by the authors, and with available wind-tunnel and full-scale experimental results. The agreement is in general good; however, the model can be improved by further refinement and adjustment of parameters. In particular, the effect of the turbulent Prandtl numbers, mainly that of the mixture fraction σ_ϵ , should be taken into account explicitly in this 1D model. For example, another 1D model, developed by Peters and Götting (1991), that is simpler than ours

gives a better agreement with the results of the 3D model than the one presented here. However, it should be stressed that this 1D model includes radiative effects in detail, whereas both in the 3D (Hernández *et al.*, 1995) model and the 1D model of Peters and Göttgens (1991) radiative losses are only contemplated in a global way. Besides, the comparison with experiments does not show conclusively that the 3D results are better than the 1D ones. Another improvement that the authors are considering is the choice of non-symmetrical profiles to take into account lateral wind and buoyancy in inclined flames. It will also be of interest to estimate the entrainment, when there is a cross wind, from the two equations giving the mechanical production of k (equations (39) and (42)), although effects such as those due to the downstream vortices and to non-symmetric profiles will have to be taken into account.

Acknowledgements

This paper relates to reaseach work carried out under contract STEP-CT90-0098 (DTEE) in the framework of the Major Industrial Hazards Research Area, with financial support of the EU. Dr. Servert had a scholarship of the Spanish Ministry of "Educación y Ciencia" within the program of "Formación de Personal Investigador".

References

- Bakkum, E. A. (1994) Physical Modelling of Jet Interaction with Vessels. JIVE final report. TNO ref. n° 94-142.
- Becker, H. A. and Liang, D. (1978) Visible Length of Vertical Free Turbulent Diffusion Flames. *Combust. Flame*, **32**, 115-137.
- Bennet, J. F. *et al.* (1991) Large Scale Natural Gas and LPG Jet Fires. Final Report to the CEC, TNER, 91, 022, Shell Research Limited.
- Birch, A. D., Hughes, D. J. and Swaffield, F. (1987) Velocity Decay of High Pressure Jets. *Combust. Sci. Technol.*, **52**, 161-171.
- Caulfield, M. *et al.* (1993) An Integral Model of Turbulent Jets in a Cross-Flow; Part 1-Gas Dispersion, Part 2-Fires. *Trans. IChemE*, **71**, 235-251.
- Cook, D. K. (1991) An Integral Model of Turbulent Non-Premixed Jet Flames in a Cross-Flow. *Twenty-Third Symposium (International) on Combustion*, The Combustion Institute, Pittsburgh, pp. 653-660.
- Crespo, A. *et al.* (1991) One-Dimensional Model of Torch Fires. UPMFIRE, companion report to Physical Modelling of Torch Fires, Final Report, from UPM to EC, contract n° EV4T-0009-E (A).
- Crespo, A. and Hernández, J. (1993) Prediction of Vertical and Horizontal Turbulent Jet Diffusion Flames in the Atmospheric Surface Layer. *The Combustion Institute. Joint Meeting of the Italian and Spanish Sections*. Stresa, Italy.
- Crespo, A., Hernández, J., Servert, J., García, J. and Manuel, F. (1994) Hazard Consequences of Jet Fire Interactions with Vessels Containing Pressurized Liquids. Final Report from UPM to EC, contract STEP-CT90-0098.

- Crespo, A., Servet, J. and Hernández, J. (1995) Application of the One-Dimensional Model UPMFIRE to Calculate Jet Fire Characteristics and its Interaction with Obstacles. *Proceedings of the 8th International Symposium on Loss Prevention and Safety Promotion in the Process Industries*. Antwerp, pp. 105–114.
- Duijm, N. J. (1993) JIVE Progress Report no. 3, TNO-IMET Report no. 93.
- Escudier, M. P. (1972) Aerodynamics of a Burning Turbulent Gas Jet in a Cross Flow. *Combust. Sci. Technol.*, **4**, 293–301.
- Fairweather, W. P. *et al.* (1991) Predictions of Radiative Transfer from a Turbulent Reacting Jet in a Cross-Wind. *Combust. Flame*, **84**, 361–375.
- Fay, J. A. (1973) Buoyant Plumes and Wakes. *Ann. Rev. Fluid. Mech.*, **5**, 151–160.
- Hernández, J., Crespo, A. and Duijm, N. J. (1995) Numerical Modeling of Turbulent Jet Diffusion Flames in the Atmospheric Surface Layer. *Combust. Flame*, **101**, 113–131.
- Modak, A. T. (1979) Radiation from Products of Combustion. *Fire Research*, **1**, 339–361.
- Mudford, N. R. and Bilger, R. W. (1984) Examination of Closure Models for Mean Chemical Reaction Rate Using Experimental Results for an Isothermal Turbulent Reacting Flow. *Twentieth Symposium (International) on Combustion*, pp. 387–394.
- Ott, S. (1993) Measurements of Temperature, Radiation and Heat Transfer in Natural Gas Flames. Final Report of the Jive Project, Riso-R-703(EN).
- Peters, N. and Göttgens, J. (1991) Scaling of Buoyant Turbulent Jet Diffusion Flames. *Combust. Flame*, **85**, 206–214.
- Ricou, F. P. and Spalding, D. B. (1961) Measurement of Entrainment by Axiallysymmetrical Turbulent Jets. *J. Fluid Mech.*, **11**, 21–32.
- Schlichting, H. (1968) *Boundary Layer Theory*, McGraw-Hill, New York.
- Servet, J. (1993) Modelado de llamas de difusión turbulenta y de su interacción con el medio ambiente y objetos circundantes. *Universidad Politécnica de Madrid, Ph. D. Thesis*.
- Servet, J., Crespo, A. and Hernández, J. (1995) A One-Dimensional Model of Jet Fires and of its Interaction with Obstacles. *Third Caribbean Congress on Fluid Dynamics*, Caracas.
- Sivathanu, Y. R. and Faeth, G. M. (1990) Generalized State Relations for Scalar Properties in Non-Premixed Hydrocarbon (Air Flames). *Combust. Flame*, **82**, 211–230.
- Tamanini, F. (1981) An Integral Model of Turbulent Fire Plumes. *Eighteenth Symposium (International) on Combustion*, pp. 1081–1090.
- Verheij, F. J. and Duijm, N. J. (1991) Windtunnel Modelling of Torch Fires. TNO Report 91-422, Apeldoorn, The Netherlands.
- Yih, C. S. (1951) Proc. of the First U. S. National Congress of Applied Mechanics, ASME. E. Stenberg, editor, pp. 941–947.